RSC Advances

PAPER

View Article Online
View Journal | View Issue



Cite this: *RSC Adv.*, 2022, **12**, 27679

# Fluorescence determination of Fe(III) in drinking water using a new fluorescence chemosensor†

Gasser M. Khairy,*[a] Alaa S. Amin,*[b] Sayed M. N. Moalla,[c] Ayman Medhat[c] and Nader Hassan[c]

Received 17th August 2022
Accepted 19th September 2022

DOI: 10.1039/d2ra05144c

rsc.li/rsc-advances

A new fluorescence chemosensor based on (*Z*)-2-(1-(3-oxo-3*H*-benzo[*f*]chromen-2-yl)ethylidene) hydrazine-1-carbothioamide (CEHC) has been developed for the determination of Fe(III) in drinking water. The optimum conditions were acetate buffer solution with a pH 5.0. In this approach, the determination of Fe(III) is based on static quenching of the luminescence of the probe upon increasing concentrations of Fe(III). The CEHC sensor binds Fe(III) in a 1 : 1 stoichiometry with a binding constant $K_a = 1.30 \times 10^4\ M^{-1}$. CEHC responds to Fe(III) in a way that is more sensitive, selective, and quick to turn off the fluorescence than to other heavy metal ions. Selectivity was proved against seven other metal ions (Mn(II), Al(III), Cu(II), Ni(II), Zn(II), Pb(II), and Cd(II)). The calibration curve was constructed based on the Stern–Volmer equation. The linear range was 2.50–150 μM with the correlation coefficient of 0.9994, and the LOD was 0.76 μM. The method was successfully applied to determine Fe(III) in drinking water samples, and the accuracy of the chemosensor was validated by atomic absorption spectrometry.

## Introduction

The field of chemical sensors is significant mainly for sensing essential metal ions in environmental and biological applications.[1,2] Chemosensors are characterized as highly sensitive, low cost, easy to perform and can be used in many different fields, which are utilized for real-time monitoring and metal ion detection in many different fields like environmental control, medical diagnostics, electronics, and live cells. One of the many analytes being studied these days is chemosensors for transition metal ions. While these ions can be harmful to the environment if present in large quantities, they are also necessary for biological systems. The three most prevalent and necessary trace elements in the human body are zinc, iron, and copper ions, which are among biologically significant metal ions and have significant functions in environment, biology, and the chemistry. Iron is the most common transition metal ion in the human body. It is an essential and important for all living cells where it acts as a cofactor in various enzymatic reactions in humans.[3] Fe(III) deficiency causes liver damage, anaemia, diabetes, Parkinson's disease, hemochromatosis, and cancer.[4] The highest permissible amount of Fe(III) in drinking water is 5.4 μM, according to the US EPA.[5]

However, it is also possible that excessive levels of redox-active iron might harm biological systems by accelerating the formation of highly reactive oxygen species,[5] which causes some kinds of diseases like cancer and Alzheimer's disease.[6–8] Therefore, the assessment of the iron concentrations is an important issue in biomedical and environmental analysis. A fatal dose of 40 mg $kg^{-1}$ has been documented in humans, and it is known to be dangerous at high concentrations.[9] The primary source of iron ions to the environment is coagulation and corrosion of ferrous materials while for humans is from drinking water and food.

Numerous techniques for determining Fe(III) have been published such as colorimetric analysis,[10] atomic absorption spectroscopy,[11,12] electrochemical,[13–15] mass spectrometry[16] and fluorescence spectroscopic analysis.[17–24] The fluorimetric assay is a popular approach because of its simplicity of use, fast time of response with simple requirements of instrumentation, high efficiency and sensitivity. Therefore, there has been an increase in interest in the development of fluorescent probes for the detection of Fe(III).[25–27] For useful applications, the probes with high-sensitivity are required because of the low concentrations of metal ions in the environment and biosystems.[28,29] Before, successful efforts were made to detect the presence of Fe(III).[30–34] However, in each instance, the selectivity is not shown for some heavy metals (that have the same features as Fe(III)) which could interfere with detection.[35] For instance, we observe that among the transition metal ions, Cu(II) bears the highest theoretical resemblance to Fe(III).[36] As a result, it is critical to thoroughly examine any Fe(III) fluorescence probe for selectivity by comparing it to other heavy metals that could exist in water,[37]

[a]*Chemistry Department, Faculty of Science, Suez Canal University, 41522 Ismailia, Egypt. E-mail: gasser_mostafa@science.suez.edu.eg*

[b]*Department of Chemistry, Faculty of Science, Benha University, Egypt. E-mail: asamin2005@hotmail.com*

[c]*Department of Chemistry, Faculty of Science, Port Said University, Egypt*

† Electronic supplementary information (ESI) available. See https://doi.org/10.1039/d2ra05144c

biological systems,[38] and the environment samples.[39] Recently, a great number of coumarin-based metal ion sensors have been described.[40] Ref. 41 provides some of the Fe(III) chemosensors. The academic literature contains an abundance of information about the coumarin derivatives regarding the synthesis[42,43] and their applications in a wide range of areas including fluorescents,[44,45] laser dyes,[46] and pharmaceuticals.[47] Since coumarins show low toxicity, high stability, and excellent optical properties,[48] we speculated that coumarin derivatives would be useful as fluorescence sensors. Many of the suggested probes lack the sensitivity and selectivity needed to detect low levels of iron ions and have a long response time. Chemical sensors' selectivity, sensitivity, and response time were greatly influenced by the type of recognition elements used in the determination method.

These procedures can represent a broad range and have significant detection limits, while the majority needed to use expensive devices in the laboratory and qualified staff for the application. However, spectrofluorometric procedures have certain advantages over sophisticated methods, such as cost, fast response time, and good precision. Alternative procedures for iron detection will undoubtedly be required instead of the conventional procedures because of the drawbacks of these methods.

In the present work, an accurate and precise spectrofluorimetric method was developed for sensing Fe(III) based on (*Z*)-2-(1-(3-oxo-3*H*-benzo[*f*]chromen-2-yl)ethylidene)hydrazine-1-carbothioamide (CEHC) as a probe. It works well as a fluorescent sensor that is very selective for Fe(III) between pH 4 and 6 relative to other interfering metal ions and most Fe(III) sensors that have been previously reported, and is straightforward, secure, affordable, ecologically friendly, and focused on green analytical chemistry. The reversibility of the probe was successfully done using EDTA solution. The outcome of this work reported a non-toxic, economical, stable, accurate, easy-to-use, and novel probe sensor material to assess Fe(III) in water samples and compared statistically with the AAS method.

# Experimental

## Reagents and chemicals

(*Z*)-2-(1-(3-oxo-3*H*-Benzo[*f*]chromen-2-yl)ethylidene)hydrazine-1-carbothioamide (CEHC) was purchased from Analytics Co. (**https://www.analytics-shop.com**). Its chemical structure is illustrated in Scheme 1. All inorganic salts were of analytical grade and obtained from Sigma-Aldrich (**https://www.sigmaaldrich.com**). All the chemicals were of analytical grade and were not purified prior to use. Chloroacetic acid and sodium chloroacetate were obtained from Merck. Acetic acid and sodium acetate were obtained from Sigma-Aldrich. Piperazine-*N*,*N*′-bis(2-ethanesulfonic acid) (PIPES), and 2-(cyclohexylamino) ethane sulfonic acid (CHES) were obtained from Sigma-Aldrich Co.

## Instrumentation

UV-VIS spectra were recorded on a Shimadzu UV-1800 UV/Visible Spectrophotometer (**https://www.shimadzu.com**) using a quartz cell with 1.0 cm of path length. The luminescence spectra were recorded with a Jasco 6300 spectrofluorometer (**https://jascoinc.com**) using a quartz cell 1.0 cm of path length and a 150 W xenon lamp for excitation. The excitation and emission bandwidths were 5 nm. The iron content in water samples was measured using PerkinElmer Model 2380 Atomic Absorption Spectrophotometer with a hollow cathode lamp of iron. A digital pH meter was used to measure the pH of the solutions (3510 Jenway, Bibby Scientific Ltd, UK), was calibrated with standard buffers of pH 7.00, 4.00 and 10.00 at 25.0 ± 1.0 °C.

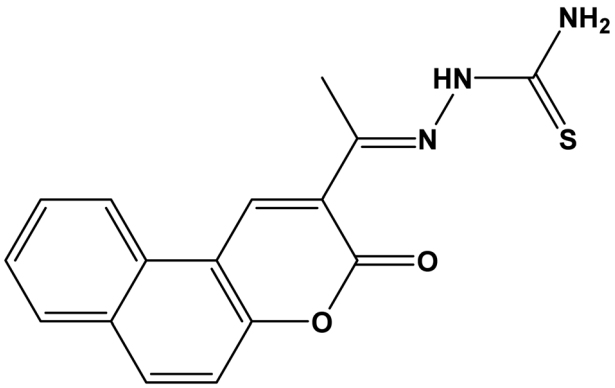


Scheme 1 The chemical structure of chemosensor (CEHC) under study.

## Solutions preparation

$1.0 \times 10^{-3}$ M stock solutions of metal ions (Fe(II), Mn(II), Al(III), Cu(II), Ni(II), Zn(II), Pb(II), and Cd(II)) were prepared using the buffer solutions to adjust the solutions. The pH was adjusted using an acetate, chloroacetate, PIPES, or CHES buffer solutions (c base + c acid = 10 mM). The $1.0 \times 10^{-3}$ M CEHC stock solutions was prepared by dissolving a certain amount in ethanol. The working solutions for studying the selectivity of the probe towards the heavy metals under our study were freshly prepared by mixing various volumes of metal ion stock solutions (0, 27, 54, 110, 190, 270, 410, 540, 680, and 810) with a fixed volume (1.0 ml) of $1.0 \times 10^{-3}$ M CEHC stock solution (1.0 ml) in a 10 ml volumetric flask. These give heavy metals concentrations of 0, 2.7, 5.4, 1.1, 1.9, 27, 41, 54, 68, and 81 μM, respectively. Finally, the solution was completed using the appropriate buffer, followed by measurement. The analysis was done through the monitoring the decrease in luminescence intensity. The quenching results were observed due to the interaction between the probe and heavy metals. The Stern–Volmer equation was used to analyze the titration data to investigate the interaction between the probe and the heavy metals under our investigation.

## Fluorescence determination procedure of Fe(III)

The luminescence spectra and intensities were monitored at the fixed analytical emission wavelength ($\lambda_{em}$ = 474 nm) of the CEHC in acetate buffer pH 5.0 using excitation wavelength =

333 nm. Fluorescence titrations were done in a 1.0 cm quartz cuvette by subsequent addition of Fe(III) (0–200 μM) to a solution of 100 μM CEHC. Fluorescence emissions were measured at room temperature after 5.0 min of incubation. The measurements were repeated thrice, and the average fluorescence intensity was calculated. The calibration curve was constructed based on the Stern–Volmer equation.

### Preparation of water samples

The samples were collected from cold and hot water pipes made of iron in a building inside our university. The water was collected after flowing for 10 min. Water samples were collected in 1000 mL plastic bottles without being treated with strong nitric acid and examined directly afterward sample digestion. 100 mL of each water sample was transferred into a 250 mL conical flask, and 10 mL of a mixture consisting of $HNO_3$ and $H_2O_2$ (1 : 9, v/v) were added. These samples were digested by heating under reflux for 1.5 h. The cooled samples were transferred into 100 mL measuring flask and made up to the mark with deionized distilled water, mixed well, then subsequently analyzed by the proposed probe and AAS methods.

## Results and discussion

### Optical characterization of (CEHC) and its interaction with Fe(III)

The optical properties of CEHC were studied by fluorescence emission spectra and UV-vis absorption spectra in acetate buffer pH = 5.0. The CEHC showed a maximum absorption wavelength at 333 nm due to the n–π* transitions ($\varepsilon_{333\ nm}$ = 16 893.88 ± 130 $M^{-1}$ $cm^{-1}$). When treated with different cations like Cu(II), Cd(II), Fe(III), Mn(II), Ni(II), Pb(II), Al(III), and Zn(II), compound CEHC showed a blue and hypochromic shift at 329 nm for Fe(III) ions proofing that the prob (CEHC) is selective to Fe(III) ions (Fig. 1). Fig. 1S† shows the fluorescent spectra of compound CEHC in the absent and presence of different metal ions. The CEHC displayed a fluorescence band at 474 nm using $\lambda_{ex}$ = 333 nm. The emission of the CEHC does not alter significantly when various metal cations are added, whereas, on the addition of Fe(III) ion, the fluorescence of CEHC was further quenched at 474 nm.

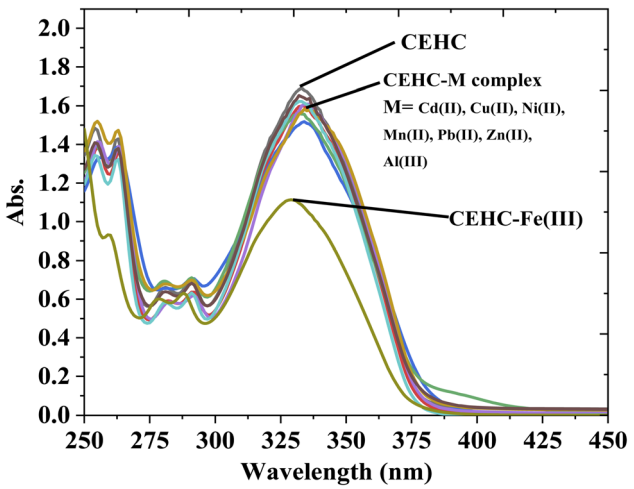


Fig. 1 UV-Vis spectra of 1 × $10^{-4}$ M of the CEHC and Fe(III) (40 μM) in absence and presence of different metal ions (40 mM) at room temperature.

It was evident that the fluorescence intensity of the CEHC was greatly quenched by Fe(III). As a result, we expected the Fe(III) added would interact with the CEHC. It is known that the Fe(III) ion is an effective fluorescence quencher because of its paramagnetic properties by energy or electron transfer.[30,49] The Fe(III) preferentially binds with oxygen and nitrogen atoms.[50,51] Thus, we deduced that, Upon the metal bonded, the oxygen atom of the carbonyl group attached to the coumarin ring and the nitrogen atom of the thiosemicarbazide group of the CEHC molecule could even donate electrons to the Fe(III). So, the molecular or/and electronic structure of the chemosensor alters. As a result, its fluorescence properties change because of a ligand–metal charge transfer (LMCT) mechanism, proving the binding of metal ion. Classification of fluorescent probes is possible based on a variety of factors. For example, based on the optical performance, the probes could be divided into ratiometric probes, "on–off" probes, and "off–on" probes. Thus, our fluorescence probe can be classified as "on–off" probe due to LMCT mechanism between CEHC and Fe(III). Detail structural and morphological characterization of Fe(II) CEHC complex based prob was represented as shown in Scheme 2.

### Binding stoichiometry and reversibility

Job's plot experiment was used to detect the CEHC–Fe(III) binding stoichiometry. Different mole fractions of Fe(III) (0.1, 0.2, 0.3, 0.4, 0.5, 0.6, 0.7, 0.8, 0.9, and 1.0) have been prepared and their fluorescence intensities have been measured. These solutions have concentrations that range from 10 μM to 100 μM. Fig. 2 show a Job's plot of a CEHC with Fe(III) ion in acetate buffer solution pH 5 at room temperature at $\lambda_{ex/em}$ = 333/474 nm. It is obvious from the plot that the minimum intensity of the luminescence occurs at a mole fraction of 0.5 of Fe(III). This finding reveals that, the binding stoichiometry between the CEHC and Fe(III) is 1 : 1.

The coordination site for the complex was confirmed by using the following observations. The infrared scanning technique provided us the presence of thiol group vibrations at 2666 $cm^{-1}$ and thione bands at 833 $cm^{-1}$ the CEHC ligand,[52] indicating that they remain as the thiol–thione tautomer forms. However, in the case of the Fe(III) complex, both types of vibrations [$\nu$(SH) and $\nu$(C=S)] were absent. It can be explained that the coordination was done through the mono-negatively charged sulfur atom *via* deprotonation of the –SH group.[52] The vibration band of the azomethine (C=N) group was shifted to a lower value by complexation, leading to the coordination of iron ion by the azomethine nitrogen. The band positions of the carbonyl groups of the ligand changed after complexation to lower values, due to the coordination of carbonyl oxygen with iron ion in the complexation process. The vibrational frequency of the optimized ligand and its Fe(III) complex was calculated, and no imaginary frequency was observed. The complete

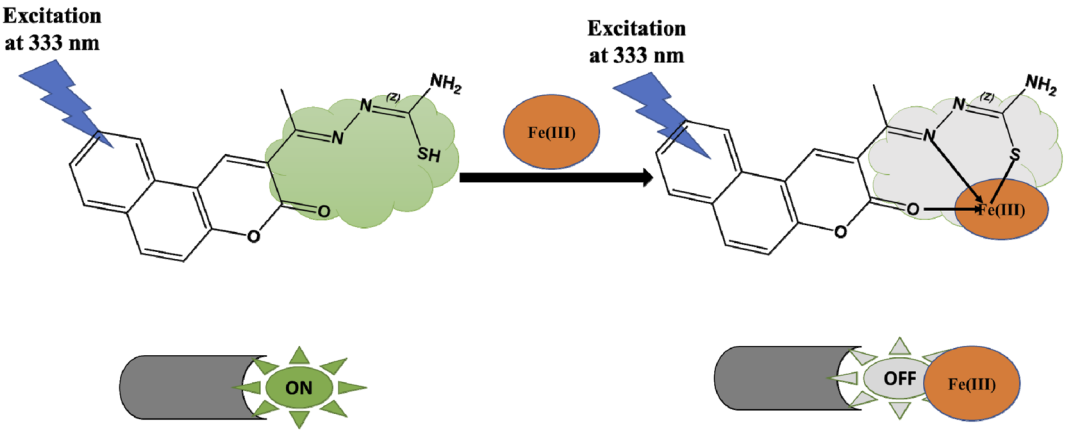


Scheme 2 Schematic representation the interaction between the probe (CEHC) and Fe(III).

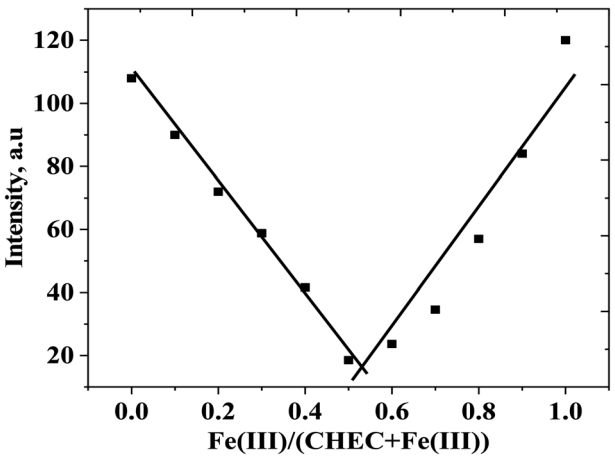


Fig. 2 Job's plot of a CEHC with Fe(III) ion in acetate buffer solution pH 5.0 at room temperature.

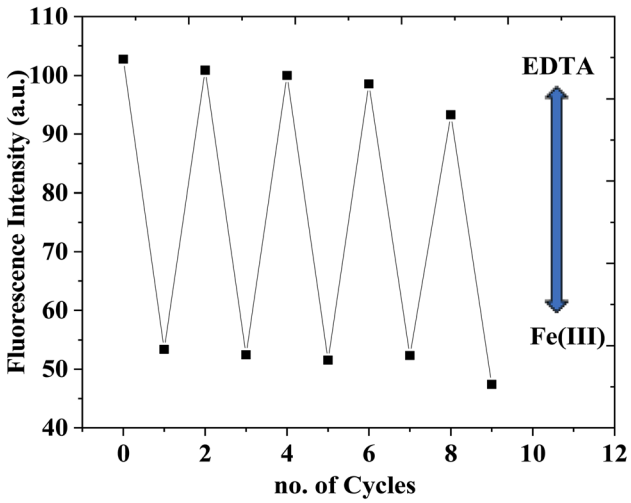


Fig. 3 Reversibility of the CEHC at fixed $\lambda_{em}$ = 474 nm after subsequent addition of 40 μM Fe(III) and EDTA.

neutralization of the complex was done by the binding with two chloride ion that was supported by the appearance of a new Fe–Cl band.[52] It is further supported by the non-electrolytic properties of the synthesized complexes. All previous coordinated bond signals observed due to (Fe–N), (Fe–O), (Fe–S) and (Fe–Cl) was presented with the most important characteristic bands.

The reversibility of the chemosensor was tested using ethylenediamine tetraacetic acid disodium salt (EDTA). On adding Fe(III) ion, the CEHC–Fe(III) was formed and the emission intensity of the CEHC was quenched. Upon treatment with EDTA, the emission of the probe enhanced due to the binding between EDTA and Fe(III) ion leaving the probe free (see Fig. 2S†). Fig. 3 shows reversibility of the CEHC at fixed $\lambda_{em}$ = 474 nm after subsequent addition of 40 μM EDTA and Fe(III). Thus, the CEHC can be considered as a reversible fluorescent chemosensor through using EDTA.

### Effect of pH

pH has a significant impact on the reagents current form and on metal chelate formation. As a result, the optimum pH for the measurements was detected by plotting the Stern–Volmer relation in the pH range 4–10 using buffer solutions with various concentration of Fe(III) from 2.7 to 81 μM. The results (Fig. 3S†) show that the optimum pH value for the measurement is 5.0, where it was observed that the slop of the curve in buffer pH = 5.0 is biggest than the slop of the curves of other pHs' values. To confirm the selectivity of CEHC toward Fe(III) ions, Stern–Volmer quenching equation was constructed for various metal ions as shown in Fig. 4S.† The resulting curves show that there is no significant variation with all the metal ions except for Fe(III) ion. The data clearly suggest that the chemosensor (CEHC) is more selective for sensing of Fe(III) ions (see also the ESI Fig. S6–S14†).

### Effect of response time

To study the response time of the chemosensor, the fluorescence intensity at 474 nm was recorded, at time interval 5.0 min for one hour and the results are shown in Fig. 5S.† For most concentrations, more than 90% of the overall signal change has happened after 5 minutes (within 1.0 hour). Due to our goal of

creating a fast Fe(III) sensing method, we set the measurement response time to 5.0 minutes.

### Effect of Fe(III) concentration

Luminescence spectra and calibration curve of 10 mM of the chemosensor (CEHC) with various concentrations of Fe(III) (0, 0.1, 0.25, 0.5, 0.75, 1, 2.5, 5, 7.5, 10, 20, 30, 50, 75, 100, 125, 150, 175, and 200 μM) in acetate buffer pH = 5, $\lambda_{ex}$ = 333 nm, at room temperature were displayed in Fig. 4a and c. The emission intensity measurements of the prob with Fe(III) displayed a quenching emission peak of the CEHC ($\lambda_{em}$ = 474 nm) with increasing the concentration of Fe(III). Examination of the $F_0/F$ against [Fe(III)] plots revealed a straight-line till 150 μM of Fe(III) reviling that the quenching process here is static quenching due to the formation of a non-fluorescent stable complex CEHC–Fe(III). At higher concentration, the plot is curvature upward reviling the quenching process changed to be dynamic quenching[65] (Fig. 4b). The association constant ($K_{sv}$) was evaluated using the Stern–Volmer equation and was found to be 1.3 × $10^4$ $M^{-1}$. The calibration plot (Fig. 4c) is based on Stern–Volmer equation. The calibration data has been collected in Table 1. The regression equation of the calibration curve is $F_0/F$ = 0.013 × [μM] + 1.01. Where $F_0$ and $F$ are the emission

Table 1 Calibration data of CEHC probe with Fe(III)

| Parameter | Fe(III) |
|---|---|
| Regression equation | $F_0/F = 0.013 \times [\mu M] + 1.01$ |
| Slop | 0.013 |
| Intercept | 1.01 |
| $R^2$ | 0.99884 |
| Accuracy ($n$ = 17) | 101.51 ± 1.57 |
| Correlation coefficient ($r$) | 0.9994 |
| Linear range | 2.5–150 μM |
| SD of intercept | 0.0008 |
| SD of intercept | 0.0033 |
| LOD | 0.76 μM |
| LOQ | 2.54 μM |

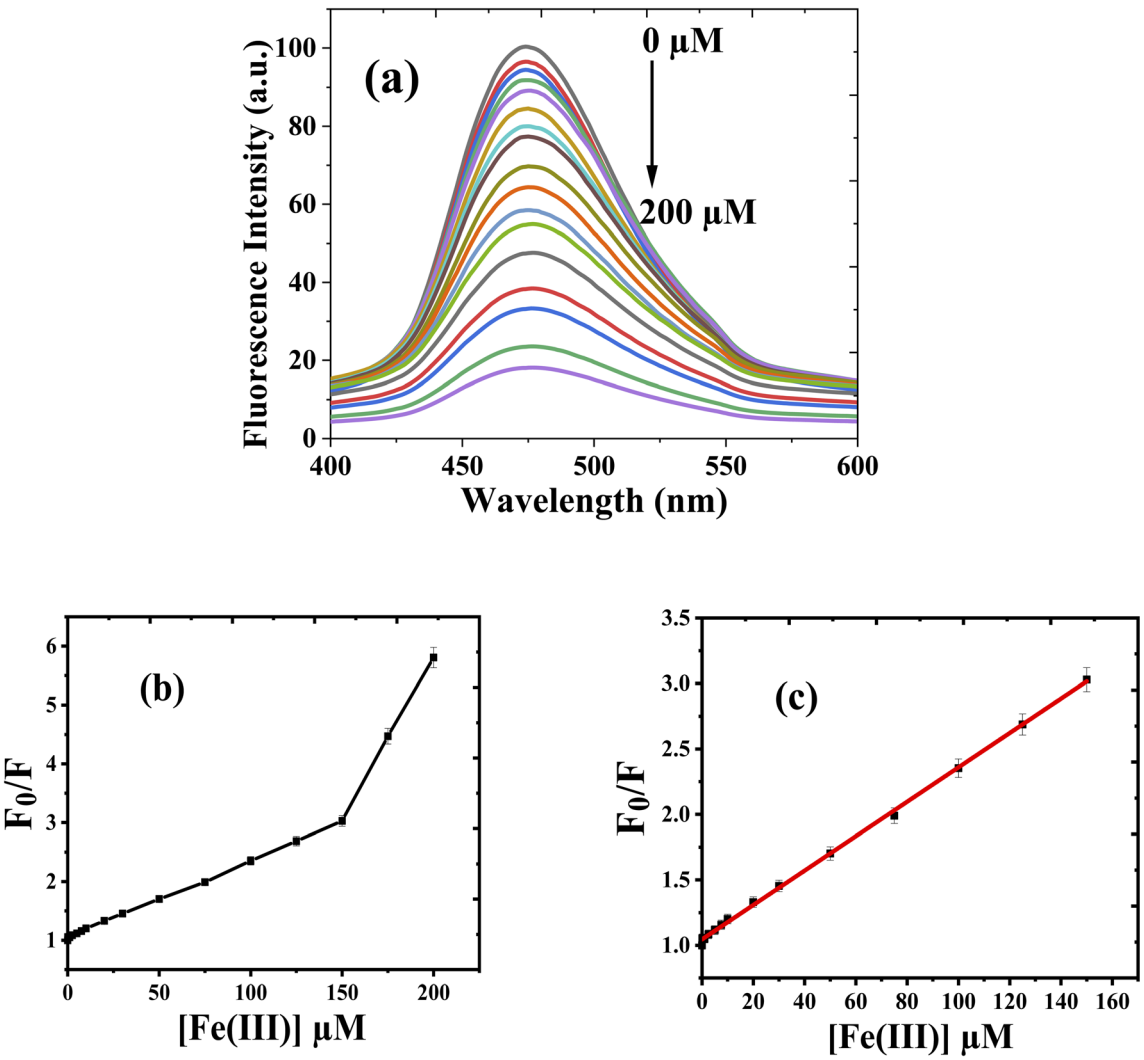


Fig. 4 (a) The fluorescence spectra (b) the Stern–Volmer plot; and (c) the calibration plot of the interaction of CEHC with various concentrations of Fe(III) ions, in acetate buffer at pH 5, $\lambda_{ex/em}$ = 333/475 nm, and room temperature.

intensities of the chemosensor before and after the addition of Fe(III). The detection limit was obtained using equation LOD = 3$\delta$/slope, in which $\delta$ is the standard deviation of the blank containing 100 μM CEHC in acetate buffer pH 5.0. The value of the detection limit was determined to be 0.76 μM. The linear range is 0.50–150.00 μM with correlation coefficient ($R^2$ = 0.9994). According to the WHO (World Health Organization) and the European Water Quality Directive,[53] the recommended Fe(III) concentration in drinking water is to be below 5.37 μM. It indicates that CEHC probe is suitable for determination the Fe(III) in drinking water. Overcoming this level could result in the progression of serious diseases. Table 2 summarizes the fluorosensors and chemosensors for determination of Fe(III). By comparing the previous methods to our proposed method, we observed that our approach is more sensitive than other methods. Furthermore, the detection limit attained by our approach is more than low enough for studying Fe(III) concentrations in environmental and biological substances. Our proposed method has a more comprehensive linear range. As a result, the most samples will not require additional dilution procedures.

### Selectivity

Probes must be able to distinguish between the analyte of interest and any other species that might be a potential competitor. Thus, the selectivity test was performed through the measurement the fluorescence change of the CEHC after the treatment of 40 μM Fe(III) ions in the existence of 40 mM other interfering metal in acetate buffer pH 5.0. From Fig. 5, We found that the detection of Fe(III) was unaffected by the presence of other metal ions. Probe (CEHC) can detect Fe(III) with minimal interference from coexisting ions, as this study showed. Thus, the CEHC prob shows a strong selectivity for Fe(III) compared to the other metal ions examined.

### Analytical application

To test the reliability of the proposed probe, it was employed to detect trace levels of Fe(III) in water samples [Table 3]. In order

Table 2 Fluorosensors and chemosensors for determination of Fe(III)

| Fluorophores/chemosensors | LOD μM | Stoichiometry | Media | Ref. |
|---|---|---|---|---|
| Rhodamine | 12.80 | 1 : 1 | Methanol/water (1/1, v/v) | 54 |
| Rhodamine | 1.20 | 1 : 1 | Water | 55 |
| Rhodamine | 50.00 | 1 : 1 | Tris HCl–$CH_3CN$ (pH 7.4) | 56 |
| Pyrene | 2.00 | 1 : 1 | DMF–HEPES (pH = 7.4) | 57 |
| Pyrene | 2.61 | 1 : 1 | $CH_3CN$ : $H_2O$ (1 : 1, v/v) | 58 |
| Pyrene | 1.42 | 1 : 1 | DMSO/$H_2O$ (pH = 7.4) | 59 |
| Pyrimidine | 12.8 | 1 : 2 | Acetonitrile (pH = 7) | 60 |
| Benzothiazole | 5.86 | 1 : 1 | DMF : $H_2O$, 1 : 1, (pH = 7.4) | 61 |
| Imidazoledete | 2.50 | 1 : 1 | Tris–HCl (pH 7.4) | 62 |
| Imidazole | 2.81 | 1 : 1 | Water | 63 |
| Acylhydrazone | 4.60 | 1 : 1 | Methanol | 64 |
| Naphthalene | 35.30 | 1 : 1 | THF/$H_2O$ (1 : 99) (pH 7.0) | 65 |
| Imine | 5.14 | 1 : 2 | DMF | 66 |
| Indole | 17.00 | — | Water | 67 |
| Bodipy | 2.59 | 1 : 2 | DMF–buffer 1/1, (v/v) | 68 |
| Phenothiazine | 4.90 | 1 : 1 | DMSO | 69 |
| Hexachlorocyclotriphosphazene | 8.04 | 1 : 2 | Water | 70 |
| Quinoxaline | 16.00 | 2 : 1 | Acetonitrile–HEPES (9 : 1, v/v, pH = 7.4) | 71 |
| Furocoumarin (furo[3,2-*c*]coumarin) derivatives | 1.93 | 2 : 1 | Methanol | 72 |
| Our chemosensor (CEHC) | 0.76 | 1 : 1 | Acetate buffer pH = 5 | This work |

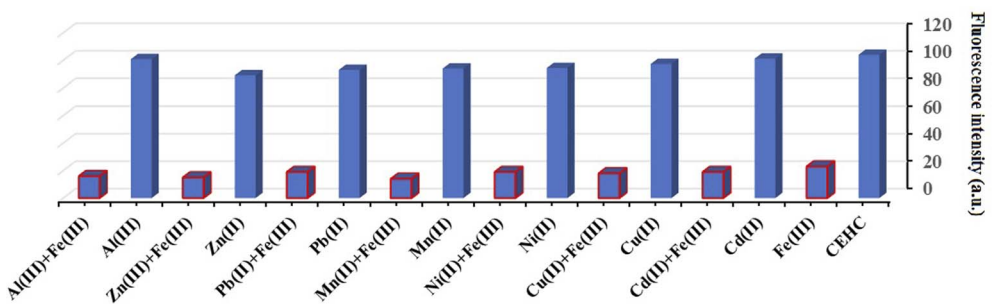


Fig. 5 Selectivity of CEHC toward Fe(III) and 40 mM other metal ions in absence (red-blue bars) and presence of 40 μM Fe(III) (blue bars) at $\lambda_{ex/em}$ = 333/475 nm in acetate buffer solution pH 5 at room temperature.

Table 3 Comparison of Fe(II) concentrations found in tap water samples using the CEHC (chemosensor) and standard method [AAS]

| | CEHC chemosensor; μM ± SD; (μg mL$^{-1}$) | | | | |
|---|---|---|---|---|---|
| Sample no. | Dilution factor | [Fe(III)] detected | Total [Fe(III)] | AAS μM ± SD; (μg mL$^{-1}$) | Recovery (%) |
| 1 | 10 | 1.12 | 11.20 ± 0.25 (0.20) | 11.93 ± 0.14 (0.213) | 106.52 |
| 2 | 10 | 4.85 | 48.50 ± 1.23 (0.866) | 47.82 ± 0.63 (0.854) | 98.60 |
| 3 | 10 | 9.23 | 92.30 ± 2.14 (1.65) | 95.65 ± 0.84 (1.708) | 103.63 |
| 4 | 10 | 20.98 | 209.80 ± 3.40 (3.75) | 203.22 ± 0.54 (3.629) | 96.86 |

to verify the accuracy of the established procedure, recovery experiments were also carried out by spiking the samples with different levels of Fe(III) before any pretreatment. Table 3 represents the obtained results. As can be seen, recoveries between 96.86 and 106.52% were achieved, which confirms the accuracy of the proposed procedure. Accuracy was assessed by comparing results with those achieved using AAS.

Using the *t*-test and *F*-value, respectively, at a 95 percent confidence interval, to check the accuracy and precision of the suggested approach, it was revealed that there is no substantial statistical variance between the gotten results.[73]

## Conclusions

According to the best of our knowledge no manufactured probe has been described in the literature for determining iron applying the studied CEHC reagent. A new and straightforward probe based on a Coumarin derivative (CEHC) was evaluated for Fe(III) using a luminescence quenching method. The static emission quenching of CEHC upon interaction with Fe(III) allows the determination by a Stern–Volmer plot in a acetate buffer solution at pH 5 in a 2.50–150 μM range. CEHC formed a 1 : 1 complex with Fe(III) and exhibited a fluorescence response of type "turn-off" to Fe(III). Selectivity experiments were done for Mn(II), Al(III), Ni(II), Cu(II), Zn(II), Cd(II), and Pb(II). CEHC was found to have a higher degree of selectivity for Fe(III) than for other interfering metal ions and most Fe(III) sensors that have been previously reported. The reversibility of the probe was successfully done using EDTA solution. Finally, the probe was accurately determined in four tap water samples, as confirmed by atomic absorption measurements.

## Data availability

All data and materials should be available upon request.

## Conflicts of interest

The authors declare that they have no conflict of interest.

## Acknowledgements

The authors are thankful to the Graduate Studies Sector at Suez Canal University for funding the research group: "Chemo- and Bio-Sensors Development for Environmental and biomedical applications".

## References

1 A. P. de Silva, H. Q. N. Gunaratne, T. Gunnlaugsson, A. J. M. Huxley, C. P. McCoy, J. T. Rademacher and T. E. Rice, *Chem. Rev.*, 1997, **97**, 1515–1566.
2 B. Valeur, *Coord. Chem. Rev.*, 2000, **205**, 3–40.
3 Y. Lu, S. M. Berry and T. D. Pfister, *Chem. Rev.*, 2001, **101**, 3047–3080.
4 N. Narayanaswamy and T. Govindaraju, *Sens. Actuators, B*, 2012, **161**, 304–310.
5 J. Annie Ho, H.-C. Chang and W.-T. Su, *Anal. Chem.*, 2012, **84**, 3246–3253.
6 L. Zecca, M. B. H. Youdim, P. Riederer, J. R. Connor and R. R. Crichton, *Nat. Rev. Neurosci.*, 2004, **5**, 863–873.
7 S. Altamura and M. U. Muckenthaler, *J. Alzheimer's Dis.*, 2009, **16**, 879–895.
8 R. Yan, J. Xu, Y. Zhang, D. Wang, M. Zhang and W. Zhang, *Chem. Eng. J.*, 2012, **200–202**, 559–568.
9 Council NR. and National Academy of Science, *Iron*, University Park Press, Baltimore, MD, 1979.
10 Y. Ma, J. Thiele, L. Abdelmohsen, J. Xu and W. T. S. Huck, *Chem. Commun.*, 2014, **50**, 112–114.
11 M. Ghaedi, K. Mortazavi, M. Montazerozohori, A. Shokrollahi and M. Soylak, *Mater. Sci. Eng., C*, 2013, **33**, 2338–2344.
12 A. S. Silva, G. C. Brandão, S. L. C. Ferreira and A. M. P. dos Santos, *Anal. Lett.*, 2022, **55**, 192–1206.
13 A. Bobrowski, K. Nowak and J. Zarębski, *Anal. Bioanal. Chem.*, 2005, **382**, 1691–1697.
14 A. Sil, V. S. Ijeri and A. K. Srivastava, *Sens. Actuators, B*, 2005, **106**, 648–653.
15 G. S. Ustabasi, C. Pérez-Ràfols, N. Serrano and J. M. Díaz-Cruz, *Microchem. J.*, 2022, **179**, 107597.
16 A. Spolaor, P. Vallelonga, J. Gabrieli, G. Cozzi, C. Boutron and C. Barbante, *J. Anal. At. Spectrom.*, 2012, **27**, 310–317.
17 L. Long, L. Zhou, L. Wang, S. Meng, A. Gong and C. Zhang, *Anal. Chim. Acta*, 2014, **812**, 145–151.
18 M. Thakur, M. Baral and B. K. Kanungo, *J. Mol. Struct.*, 2022, **1248**, 131436–131453.
19 H. Sheng, X. Meng, W. Ye, Y. Feng, H. Sheng, X. Wang and Q. Guo, *Sens. Actuators, B*, 2014, **195**, 534–539.
20 A. Shahat, N. Y. Elamin and W. Abd El-Fattah, *ACS Omega*, 2022, **7**, 1288–1298.

21 M. Saleem, R. Abdullah, A. Ali, B. J. Park, E. H. Choi, I. S. Hong and K. H. Lee, *Bioorg. Med. Chem.*, 2014, **22**, 2045–2051.
22 R. Wang, F. Yu, P. Liu and L. Chen, *Chem. Commun.*, 2012, **48**, 5310–5312.
23 M. Thakur, M. Baral and B. K. Kanungo, *J. Mol. Struct.*, 2022, **1248**, 131436–131453.
24 S. Mahata, G. Janani, B. B. Mandal and V. Manivannan, *J. Photochem. Photobiol., A*, 2021, **417**, 113340–113351.
25 K. P. Carter, A. M. Young and A. E. Palmer, *Chem. Rev.*, 2014, **114**, 4564–4601.
26 Y. Yang, Q. Zhao, W. Feng and F. Li, *Chem. Rev.*, 2013, **113**, 192–270.
27 S. Maher, B. Bastani, B. Smith, F. Jjunju, S. Taylor and I. S. Young, in *IEEE SENSORS*, IEEE, 2016, pp. 1–3.
28 J. Zhang, F. Cheng, J. Li, J.-J. Zhu and Y. Lu, *Nano Today*, 2016, **11**, 309–329.
29 O. García-Beltrán, B. Cassels, C. Pérez, N. Mena, M. Núñez, N. Martínez, P. Pavez and M. Aliaga, *Sensors*, 2014, **14**, 1358–1371.
30 G. F. Chen, H. M. Jia, L. Y. Zhang, J. Hu, B. H. Chen, Y. L. Song, J. T. Li and G. Y. Bai, *Res. Chem. Intermed.*, 2013, **39**, 4081–4090.
31 B. Zhao, T. Liu, Y. Fang, L. Wang, B. Song and Q. Deng, *Tetrahedron Lett.*, 2016, **57**, 4417–4423.
32 J. Yao, W. Dou, W. Qin and W. Liu, *Inorg. Chem. Commun.*, 2009, **12**, 116–118.
33 W. Wang, J. Wu, Q. Liu, Y. Gao, H. Liu and B. Zhao, *Tetrahedron Lett.*, 2018, **59**, 1860–1865.
34 R. Wang, Q. Wan, F. Feng and Y. Bai, *Chem. Res. Chin. Univ.*, 2014, **30**, 560–565.
35 X. Liu, N. Li, M.-M. Xu, J. Wang, C. Jiang, G. Song and Y. Wang, *RSC Adv.*, 2018, **8**, 34860–34866.
36 A. J. Weerasinghe, F. A. Abebe and E. Sinn, *Tetrahedron Lett.*, 2011, **52**, 5648–5651.
37 I. Sato, H. Kudo and S. Tsuda, *J. Toxicol. Sci.*, 2011, **36**, 829–834.
38 G. Szczepaniak, W. Nogaś, J. Piątkowski, A. Ruszczyńska, E. Bulska and K. Grela, *Org. Process Res. Dev.*, 2019, **23**, 836–844.
39 O. Masson, G. Steinhauser, D. Zok, O. Saunier, H. Angelov, *et al.*, *Proc. Natl. Acad. Sci.*, 2019, **116**, 16750–16759.
40 D. Cao, Z. Liu, P. Verwilst, S. Koo, P. Jangjili, J. S. Kim and W. Lin, *Chem. Rev.*, 2019, **119**, 10403–10519.
41 S. Chakraborty, M. Mandal and S. Rayalu, *Inorg. Chem. Commun.*, 2020, **121**, 108189–108212.
42 F. G. Medina, J. G. Marrero, M. Macías-Alonso, M. C. González, I. Córdova-Guerrero, A. G. Teissier García and S. Osegueda-Robles, *Nat. Prod. Rep.*, 2015, **32**, 1472–1507.
43 K. K. Aslam, M. K. K. Khosa, N. Jahan and S. Nosheen, *Pak. J. Pharm. Sci.*, 2010, **23**, 449–454.
44 H. A. Azab, G. M. Khairy and R. M. Kamel, *Time-resolved fluorescence sensing of pesticides chlorpyrifos, crotoxyphos and endosulfan by the luminescent Eu(III)–8-allyl-3-carboxy-coumarin probe*, Elsevier B.V., 2015, vol. 148.
45 H. A. Azab, G. M. Khairy and R. M. Kamel, *Spectrochim. Acta, Part A*, 2015, **148**, 114–124.
46 G. Bakhtiari, S. Moradi and S. Soltanali, *Arabian J. Chem.*, 2014, **7**, 972–975.
47 P. K. Jain and H. Joshi, *J. Appl. Pharm. Sci.*, 2012, **2**, 236–240.
48 S. M. Sethna and N. M. Shah, *Chem. Rev.*, 1945, **36**, 1–62.
49 Z. M. Anwar, I. A. Ibrahim, R. M. Kamel, E. T. Abdel-Salam and M. H. El-Asfoury, *J. Mol. Struct.*, 2018, **1154**, 272–279.
50 A. J. Weerasinghe, F. A. Abebe and E. Sinn, *Tetrahedron Lett.*, 2011, **52**, 5648–5651.
51 M. H. Lee, T. van Giap, S. H. Kim, Y. H. Lee, C. Kang and J. S. Kim, *Chem. Commun.*, 2010, **46**, 1407–1409.
52 A. I. Matesanz, J. M. Pérez, P. Navarro, J. M. Moreno, E. Colacio and P. Souza, *J. Inorg. Biochem.*, 1999, **76**, 29.
53 F. Edition, *World Health*, 2011, **1**, 104–108.
54 Z. Wu, Z. Xu, H. Tan, X. Li, J. Yan, C. Dong and L. Zhang, *Spectrochim. Acta, Part A*, 2019, **213**, 167–175.
55 J. Wang, L. Long, G. Xiao and F. Fang, *Open Chem.*, 2018, **16**, 1268–1274.
56 N. R. Chereddy, S. Thennarasu and A. B. Mandal, *Dalton Trans.*, 2012, **41**, 11753–11759.
57 Y. Guo, L. Wang, J. Zhuo, B. Xu, X. Li, J. Zhang, Z. Zhang, H. Chi, Y. Dong and G. Lu, *Tetrahedron Lett.*, 2017, **58**, 3951–3956.
58 S. D. Padghan, A. L. Puyad, R. S. Bhosale, S. V. Bhosale and S. V. Bhosale, *Photochem. Photobiol. Sci.*, 2017, **16**, 1591–1595.
59 H.-T. Tsai, Y. R. Bhorge, A. J. Pape, S. N. Janaki and Y.-P. Yen, *J. Chin. Chem. Soc.*, 2015, **62**, 316–320.
60 S. S. Mati, D. Singharoy, B. Samai, S. Konar, N. Santra, S. Pal, P. Das and S. Murmu, *J. Mol. Struct.*, 2019, **1184**, 102–109.
61 X. Gong, X. Ding, N. Jiang, T. Zhong and G. Wang, *Microchem. J.*, 2020, **152**, 104351–104360.
62 Y. Zhao, G. Zhang, Z. Liu, C. Guo, C. Peng, M. Pei and P. Li, *J. Photochem. Photobiol., A*, 2016, **314**, 52–59.
63 S. Bishnoi and M. D. Milton, *J. Photochem. Photobiol., A*, 2017, **335**, 52–58.
64 Y. Li, W. Pan, C. Zheng and S. Pu, *J. Photochem. Photobiol., A*, 2020, **389**, 112282–112289.
65 H. J. Jung, N. Singh, D. Y. Lee and D. O. Jang, *Tetrahedron Lett.*, 2010, **51**, 3962–3965.
66 D. Akram, I. A. Elhaty and S. S. Al-Neyadi, *Chemosensors*, 2020, **8**, 1–13.
67 M. R. G. Fahmi, Y. S. Kurniawan, L. Yuliati and H. O. Lintang, *Proceedings of the 5th International Symposium on Applied Chemistry*, 2019, pp. 020062–020069.
68 C. Li, Q. Sun, Q. Zhao and X. Cheng, *Spectrochim. Acta, Part A*, 2020, **228**, 117720–117729.
69 S. Santharam Roja, A. Shylaja and R. Kumar, *ChemistrySelect*, 2020, **5**, 2279–2283.
70 A. Uslu, E. Özcan, S. O. Tümay, H. H. Kazan and S. Yeşilot, *J. Photochem. Photobiol., A*, 2020, **392**, 112411–112418.
71 S. Chakraborty, S. Goswami, C. K. Quah and B. Pakhira, *R. Soc. Open Sci.*, 2018, **5**, 180149.
72 N. M. Sarih, A. Ciupa, S. Moss, P. Myers, A. G. Slater, Z. Abdullah, H. A. Tajuddin and S. Maher, *Sci. Rep.*, 2020, **10**, 7421–7431.
73 J. N. Miller and J. C. Miller, *Statistics and Chemometrics for Analytical Chemistry*, Prentice-Hall, London, 5th edn, 2005.